Journal of Rock Mechanics and Geotechnical Engineering. 2011, 3 (3): 260–269

Journal of Rock Mechanics and Geotechnical Engineering

Journal online: www.rockgeotech.org

Prospect of HDR geothermal energy exploitation in Yangbajing, Tibet, China, and experimental investigation of granite under high temperature and high pressure

Yangsheng Zhao[1*], Zijun Feng[1], Baoping Xi[1], Jinchang Zhao[1], Zhijun Wan[2], Anchao Zhou[1]

[1] *College of Mining Engineering, Taiyuan University of Technology, Taiyuan, 030024, China*

[2] *School of Mines, China University of Mining and Technology, Xuzhou, 221008, China*

Received 14 February 2011; accepted in revised form 19 July 2011; accepted 25 July 2011

Abstract: Hot dry rock (HDR) geothermal energy, almost inexhaustible green energy, was first put forward in the 1970s. The development and testing of HDR geothermal energy are well reported in USA, Japan, UK, France and other countries or regions. In this paper, the geological characters of Yangbajing basin were first analyzed, including the continental dynamic environments to form HDR geothermal fields in Tibet, the tectonic characteristics of south slope of Nyainqêntanglha and Dangxiong-Yangbajing basin, and the in-situ stresses based on the investigations conducted, and then the site-specific mining scheme of HDR geothermal resources was proposed. For the potential development of HDR geothermal energy, a series of experiments were conducted on large-scale granite samples, 200 mm in diameter and 400 mm in length, at high temperature and high triaxial pressure for cutting fragmentation and borehole stability. For the borehole stability test, a hole of 40 mm in diameter and 400 mm in length was aforehand drilled in the prepared intact granite sample. The results indicate that the cutting velocity obviously increases with temperature when bit pressure is over a certain value, while the unit rock-breaking energy consumption decreases and the rock-breaking efficiency increases with temperature at the triaxial pressure of 100 MPa. The critical temperature and pressure that can result in intensive damage to granite are 400–500 °C and 100–125 MPa, respectively.

Key words: hot dry rock (HDR); geothermal energy exploitation; high temperature and high pressure; cutting fragmentation; borehole stability

1 Introduction

The geothermal resources reserved in rocks with temperature over 200 °C are basically deemed as high-temperature rock geothermal resources, which are also named as hot dry rock (HDR) geothermal energy by the scientists from Los Alamos National Laboratory, USA. The total HDR geothermal reserve within the depth of 10 km in earth's crust is (40–400) × 10^6 quads (1 quad = 1.055×10^{18} J), which is equal to 100–1 000 times of the total fossil energy [1–3]. As reported, there are abundant HDR geothermal resources in China. The abnormal geothermal zones of HDR have been formed in Qinghai-Tibet Plateau due to the subduction zone of Indian Ocean Plate to continent of Europe in Southwest China, such as the typical abnormal geothermal zones in Yangbajing basin in Tibet and Tengchong in Yunnan Province. In Southeast China, the high geothermal gradient zones are concentrated in Taiwan, Hainan provinces and southeast coastal area along the tectonism of Philippine Plate. And there also exist dormant volcanoes or vulcanian eruption zones, such as Changbai Mountain, Wudalianchi, etc., and high geothermal gradient zones, such as Tianjin, Beijing, and Shandong Province [4], etc.

The natural hot water resources in the Yangbajing zone in Tibet, China, have been obviously reduced for the last 20 years' exploitation. The temperature, pressure and flow rate of production wells in this zone have declined to some extent. As expected, the geothermal resources in the Yangbajing zone can provide energy for a 16-MW geothermal power station at full load operation.

Geophysical exploration indicates that there exists a liquation magma chamber, outer temperature of which is about 500 °C at the depth of 5–15 km in the Yangbajing geothermal field. The geothermal gradient is about 45 °C/km. The reservoir is mainly composed of granite layer and it is high-gradient HDR geothermal resources. The current exploitation of

Doi: 10.3724/SP.J.1235.2011.00260

*Corresponding author. Tel: +86-351-6018893; E-mail: y-s-zhao@263.net

resources is basically using shallow hot water, which is only a small proportion of geothermal reserves in the Yangbajing geothermal field. Therefore, exploitation and use of HDR geothermal resources in the deep Yangbajing geothermal field are a preferred choice for replacement of shallow hot water and it can increase the electrical capacity of Yangbajing geothermal power station.

However, the fist problem encountered in the HDR thermal energy exploration is to drill rocks in geothermal reserves area at high temperature and high pressure (HTHP). Polycrystalline diamond compact (PDC) coring bit developed for HDR exploitation by Japanese scientists in the 1990s could drill the stratum at 250 °C at a depth of 1 900 m [5, 6]. Zhao et al. [7] studied the cutting effects of granite under coupled dynamic-static loads. Yet, the tests were conducted only at normal temperature and pressure, but not at HTHP.

Problems of borehole necking and collapse, resulting from drastic decline in intensity and rheology of rock mass at HTHP, are extremely serious during drilling. And the costs for drilling and preserving borehole stability will largely be increased. So the investigations on borehole stability are urgently needed. But recent reports on borehole stability were basically focused on developing diverse models at normal temperature and pressure [8–11], or discussing the micromechanisms of borehole instability based on drilling experiments conducted on a variety of granites, limestones and sandstones at room temperature [12].

In this paper, the HDR geothermal reserves are first estimated, and the technical schemes for HDR geothermal energy exploitation are presented based on temperature distribution in the Yangbajing geothermal field and the character of tectonic stress. Then experiments are conducted on granite samples with 200 mm in diameter and 400 mm in length at HTHP for rock breaking and borehole stability, using 600 °C 20 MN servo-controlled triaxial rock testing machine.

2 Technical schemes for HDR geothermal energy exploitation

2.1 Temperature distribution and geothermal resources evaluation

Dangxiong-Yangbajing basin is a long and narrow downfaulted basin and its orientation is NE. It is located in the southeast of Nyainqêntanglha and connected with Brahmaputra seam in the south. This area can be divided into two parts by China-Nepal road. In the south, the superficial formation is Quaternary alluvium. And it is moraine deposit, accompanied by weathered granite with different thickness [13]. There are a number of extensional faults, which control the strike of the basin.

Results obtained by using artificial seismic wave method show that a low-velocity layer, which is possible underground magma, exists in the depth of 22 km in the Yangbajing geothermal field. Based on the results of magneto-electrotelluric exploration (METE), there is a low-resistance (5 Ω·m) layer, which is referred as melt mass after high temperature cooling (Fig.1), at the depth of around 5 km in the north of the Yangbajing geothermal field. According to the data of deep seismic reflection exploration, there is a local liquating rock mass at the depth of 13–22 km of the supracrust in the north of Yangbajing geothermal field [14]. So it is confirmed that a heat producer induced by the high-temperature liquating magma exists in the deep layer of the Yangbajing geothermal field.

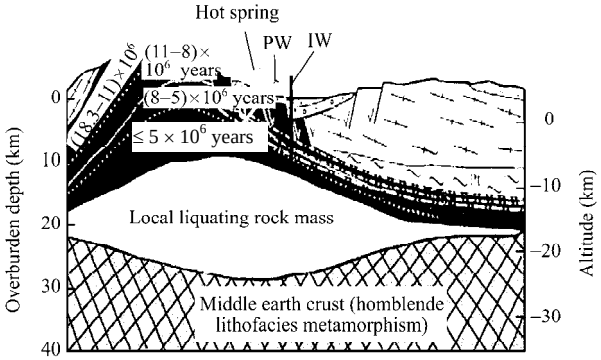

Fig.1 Crustal structure and tectonic model of Dangxiong-Yangbajing basin (PW represents production well, and IW injection well).

According to isotope analysis of hydrogen and oxygen from the thermal groundwater, the general replenishing height of the hot water, which consists of modern atmospheric precipitation and surface water infiltration, is 4 860 m, just equal to the elevation of local snowline and original distribution of surface water system. Large amount of snow-melting water from Nyainqêntanglha range and atmospheric precipitation permeates underground along the fault belts, and deep water-bearing stratum can get sustainable water replenishment continually. It will absorb the rock's heat by heat exchange with the hot rocks in the cycle. Meanwhile, the density difference of hot and cool water can produce natural upwelling, making the flow move upward along the faults. So a high-temperature thermal storage can be formed in a

relatively closed fissure system. If this flow is hindered, the hot water will spread southeast forward, and then the main flow will move from northwest to southeast to form a shallow layer thermal storage, as shown in Fig.2.

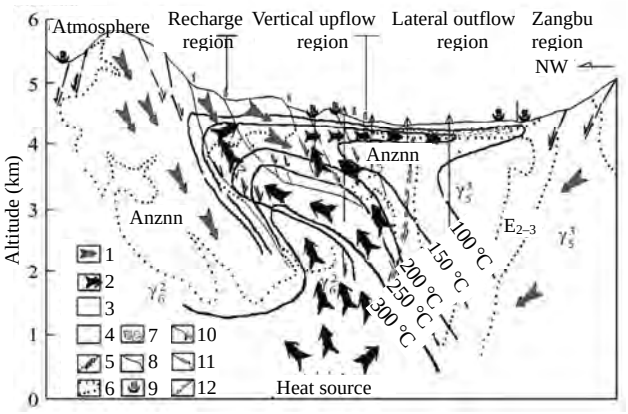

1—make-up water from atmosphere; 2—thermal upflow water; 3—temperature isoline; 4—Quaternary system porous-type heat reservoir; 5—bedrock porous-type superficial heat reservoir; 6—deep stratoid bedrock fracture-type high temperature heat reservoir; 7—boiling spring; 8—vapor ground; 9—geological boundary; 10—slide-disunion fault plane; 11—normal fault; 12—blind fault

Fig.2 Yangbajing geothermal field and hot water cycle.

According to the vertical distribution of morphology and the characteristics of deep-seated liquating mass revealed in the Yangbajing geothermal field, the temperature field distribution in this geothermal zone is analyzed by finite element method, as shown in Fig.3 [15]. From Fig.3, it can be observed that the temperature of deep-seated liquating rock masse in Nyainqêntanglha is more than 500 °C. The horizontal distance of the temperature field is approximately 180 km, while 20 km in the vertical direction. The geothermal gradient is about 45 °C/km in the vertical direction.

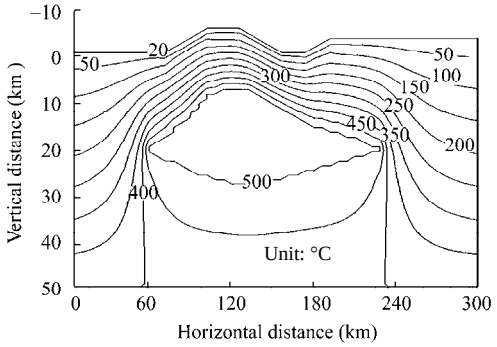

Fig.3 Finite element analysis results of temperature distribution in Dangxiong-Yangbajing basin [15].

According to Wu et al. [16], the distribution length of deep-seated liquating mass in the northeast of the Yangbajing geothermal field is over 150 km. Therefore, the liquating mass geothermal resources can be calculated within the depth of 7–18 km. In this way, the sectional area of 1 200 km^2 can be calculated by dividing the mass into many small zones. Thus, the total volume of the mass is 180 000 km^3 and its average temperature that can be measured is 500 °C. If the lowest temperature is 150 °C, the total geothermal reserve will be 5.4×10^9 MW·h per year. If the electrical efficiency is considered to be 0.17, the energy output will be 0.92×10^9 MW·h per year. This can supply a power station with an installed capacity of 50 000 MW for 1.8×10^4 years. It is obvious, as a great potential green energy, that the geothermal energy will become optimum substitution energy in China.

2.2 Characteristics of tectonic stress field in the Yangbajing geothermal field

The exploration and use of geothermal resources from deep-seated thermal reservoir in the Yangbajing geothermal field are immediately influenced by the recent crustal stress state. Therefore, it is necessary to study the characteristics of crustal stress field. Zhang et al. [17] measured the crustal stress by piezomagnetic stress relief method. They set four testing points in the Yangbajing geothermal field, two of which, (Ybj1, Ybj2), were put at the right side of Duilongqu and the other two (Ybj3, Ybj4) at the left side of the road G109. The tested lithology of strata is middle coarse-grained granite with joints and fissure developed on the ground surface, but the deep rock strata are intact. The measured results of crustal stress indicated that the direction of the maximum horizontal principal stress in the Yangbajing zone is NE-NEE and its value is between 3.3 and 10.4 MPa, while the minimum horizontal principal stress ranges from 2.5 to 8.4 MPa.

Based on the focal mechanism solution [18], although the directions of compressive and tensile principal stresses in the middle south of Qinghai-Tibet Plateau correspond to the entire feature of Tibetan Plateau, the earthquake type, which belongs to normal fault type induced by the EW force, is different from the extrusion reversed fault type of surrounding plateau induced by compressive stress. Especially, in the vicinity of the Yangbajing high heat flow zone, the EW stress field is dominant in the lithosphere stress field and its inferred control depth may be greater than 100 km. A series of large normal fault activities induced by expansion of EW lithosphere due to the effect of EW tectonic stress in the abnormal geothermal field in Qinghai-Tibet Plateau result in a high temperature heat flux in deep asthenosphere, upward along the active normal faults. Thus, the fractures are formed and then the abnormal high temperature geothermal zone is

generated.

The measured results of crustal stress and focal mechanism solution analysis show that the minimum and the maximum horizontal principal stresses in the Yangbajing geothermal field are perpendicular and parallel to the basin strike, respectively. These characteristics of modern crustal stress field are consistent with fracture of rock masses occurring in the southeast of Nyainqêntanglha. It is indicated that the original and modern tectonic stress fields have the same characters, providing scientific basis for design and development of deep HDR geothermal resources according to the characteristics of geological tectonic stress and orientation.

2.3 Design of HDR geothermal resources exploitation

Based on the characteristics of HDR geothermal energy in the Yangbajing basin shown in Fig.1 and developing tectonic characteristics of huge rock masses between the south slope of Nyainqêntanglha and Dangxiong-Yangbajing basin, five huge normal faults are developed with a large inclination, 55°–70° at the depth of 5–6 km or above ground from the mountain top of Nyainqêntanglha to Dangxiong-Yangbajing basin. The extension distance of these faults is 4–6 km. At the same time, there exist a number of small fractures with the same dip along the strike of Dangxiong-Yangbajing basin in NE direction. Both the results of in-situ stress and analysis of focal mechanism solution show that the minimum horizontal principal stress is perpendicular to these faults and fissure planes.

These faults gradually induce many shear zones or sliding bands with a mild inclination of 15°–20°, having the same strike as the outline of magma pocket when the depth exceeds 6 km. The distance between fault plane and ground surface gradually increases from Nyainqêntanglha to Dangxiong-Yangbajing basin and then to Pangduo mountain, as shown in Fig.4. The fault F5 is located in the centre of Yangbajing basin, and the other faults, F4, F3, F2 and F1, are distributed from Yangbajing basin to the south side of Nyainqêntanglha.

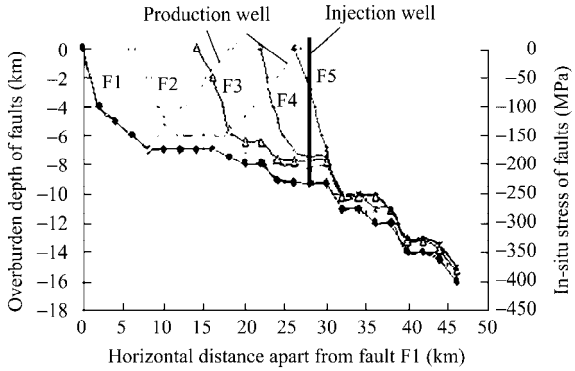

Fig.4 Change of faults overburden depth, injection and production wells with the arrangement.

2.3.1 *Design of mining project on HDR geothermal resources in Yangbajing basin*

Based on the analysis of geological structure in the Yangbajiing basin, the mining program is proposed. A vertical water injection well is constructed at a depth of 9 000 m in the horizontal centre of the faults between F5 and F4. The distance from the fault F1 is 27–28 km, as shown in Fig.4. Well cementation is constructed at the point 8 500 m from the ground surface, and the residual length of 500 m, i.e. from 8 500 to 9 000 m underground, is open wellbore or protected with shock tube. Two inclined shafts are also constructed as production wells in the north of the water injection well shown in Fig.1, and they pass through the faults F1, F2, F3 and F4. Thus, a rounded mining system, composed of the water injection well, the production wells and the faults F1 to F5, is established. In Figs.1 and 4, the temperature of the horizontal shear zones of the faults, passing through the water injection and production wells, ranges from 350 °C to 450 °C. The distance from liquating magma pocket to the system is 500–1 000 m.

2.3.2 *Construction of artificial reserve and evaluation of HDR geothermal resources*

As shown in Fig.1, the vertical distance between the injection and production wells in the mining scope of the geothermal energy is 4 km, while the length of inclination is 25 km and the horizontal spreading range is around 3 km. Thus, the total volume of fractured rocks, considered as artificial reserve of HDR geothermal resources, amounts to 3×10^{11} m^3. It is 360 times greater than that in hydrofracturing in Cornwall, British (8.25×10^8 m^3), and 973 times greater than that in Soultz, France, for HDR geothermal mining [19–23]. The natural tectonic zone considered as artificial reserve has certain advantages, and it is the basic for the mining design proposed in this paper.

Moreover, due to the minor horizontal principal stress perpendicular to the fault plane, the expansion direction of fissures is also perpendicular to the direction of the minor horizontal principal stress. Therefore, both initial and newly formed fissures are throughly intersectant with the production well, which is favorable for the discharge of superheated steam from the production well to ground surface.

The controlled resources in this mining system may be calculated as follows:

$$Q = \rho VcT \quad (1)$$

where Q is the minable energy resource (8.76×10^3 kW·h), ρ is the density of granite (2 700 kg/m^3), V is the volume of artificial reserve (m^3), c is the specific heat capacity of granite (1 000 J·kg^{-1}·°C^{-1}), and T is the temperature of extracted thermal energy (°C). The calculated result of Q is 5.62×10^{13} kW·h. If the thermal use ratio is 17%, the electric energy production will reach 9.55×10^{12} kW·h. Therefore, the energy can provide a power station with an installed capacity of 10 000 MW to work for 109 years. If the transportation of HDR geothermal energy from liquating magma pocket is considered during mining, the geothermal resources extracted from this zone will be four times at least as much as that calculated by Eq.(1). However, at the beginning of construction, a power station with an installed capacity of 1 000 MW should be built for minimal initial investment, and initial production capacity of the extracted geothermal energy.

3 Experiments on granite samples for rock breaking and borehole stability

3.1 Rock samples

Six granite samples (three for each test), Luhui granite from Shandong Province in China, were selected for experimental study of rock breaking and borehole stability. All samples were cored from a large rock block with irregular shape in a rock quarry in Pingyi, Shandong Province. They were first cut into cylinders roughly by stone processing machine and then were lathed carefully with dimensions of 200 mm in diameter and 400 mm in length, according to experimental precision. The Luhui granite is composed of 25% illite, 28% quartz, 43% feldspar and 4% others. The grain size of quartz is 0.6–0.7 mm and that of feldspar is 1–2 mm. The initial porosity is 0.30%–0.55%. A hole of 40 mm in diameter and 400 mm in length was aforehand drilled at the center of each samples for borehole stability analysis (Fig.5).

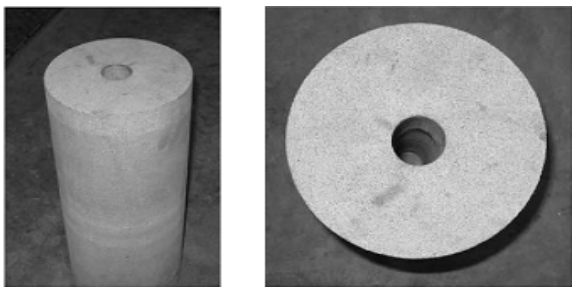

Fig.5 Granite samples with a hole at the center with dimensions of 40 mm in diameter and 400 mm in length.

3.2 Experimental apparatus and procedures

3.2.1 *Main loading apparatus*

All experiments were performed on 20 MN servo-controlled triaxial rock testing machine, as shown in Fig.6. The testing machine was developed by the authors in China University of Mining and Technology. The testing machine basically includes three units: host loading system, auxiliary system for sample assembly and measurement system. The host loading system can control and measure temperature, pressure and deformation of samples during testing. All samples are assembled before testing on the auxiliary system, which is independent but connected by guide rail with host loading system. The temperature, pressure and deformation are recorded automatically by controlling computer. A sample is assembled in the HTHP vessel before test starts. The confining pressure is transmitted by sodium chloride solid, and the axial pressure is directly exerted on the sample end through a transmitted pressure steel cylinder. The axial pressure and confining pressure can be loaded on the sample separately. According to Bai and Wang [24], the confining pressure is uniform at room temperature for the triaxial testing apparatus with solid confining medium. But the decisive factor for the axial pressure is the friction between solid confining medium and sample, and it can be approximately eliminated by holding axial pressure and confining pressure at the same time. Thus, the stresses applied to the sample are stable and reliable. The deformation of the tested samples can be precisely measured by grating sensor with a precision of 0.005 mm. Thermocouples are applied to measure the sample's temperature. The maximum axial and lateral loads both are 10 MN, which can simulate the depth of about 10 km underground. The maximum axial pressure reaches 318 MPa, while the lateral pressure is 250 MPa. The dimensions of tested sample are basically 200 mm in diameter and 400 mm in length. Its volume is approximately 64 times that of a standard sample. The

Fig.6 20 MN servo-controlled triaxial rock testing machine.

maximum temperature of the testing machine is not less than 600 °C. The whole stiffness of the equipment is not less than 14.8×10^{10} N/m.

3.2.2 *Drilling system*

The drilling system seated on the top of host loading system consists of controlling system and boring bar rotating system (Figs.6 and 7). The controlling system is considered to adjust the frequency of rotating electric motor and bit pressure (BP). The vertical gear driving the boring is driven by the horizontal gear of electric motor. The rotating speed of boring bar can be calculated according to the rotating speed of the electric motor and the gear ratio of horizontal gear to vertical gear. The BP is controlled by adjusting the flow of hydraulic cylinder. The torsion value is automatically recorded by a torque meter.

1—hydraulic cylinder for BP; 2—percussive drilling weight; 3—percussion electric motor; 4—boring bar slot; 5—rotating electric motor; 6—horizontal gear; 7—vertical gear

Fig.7 Drilling system employed in the tests.

3.2.3 *Borehole deformation measurement system*

The high temperature displacement transducer (HTDT) and TS-3800 static resistance strain transducer (SRST) were applied to measuring the borehole deformation at temperature up to 240 °C. A new apparatus (Fig.8) was developed based on the principle of optics to observe the displacement of borehole at temperature above 240 °C since the resistance of HTDT was greatly reduced by high temperature. The new optical visualizer independent of temperature has an amplification factor of 120 and a precision of 0.001 mm. A displacement tracker was fixed in the middle of the borehole. When the borehole deforms, the tracker will move. We can observe the displacement of the tracker through the optical apparatus shown in Fig.8. Thus, the borehole deformation can be calculated according to the tracker displacement.

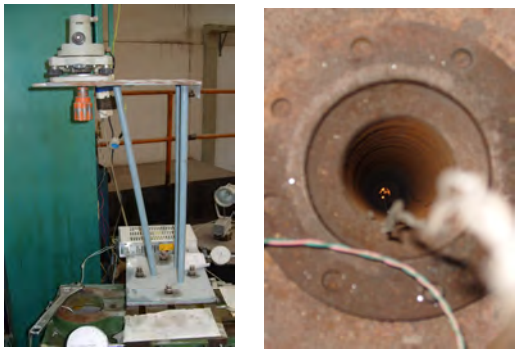

Fig.8 Optical apparatus for the observation of borehole deformation.

3.2.4 *Experimental procedure*

All samples were assembled in the HTHP vessel of the auxiliary system before tests, and then the vessel was driven along the guide rail on the platform of host loading system (Fig.6). The temperature and pressure were applied to the samples by the host loading system and deformation was measured.

The first granite sample for rock breaking was tested under a hydrostatic pressure of 100 MPa (around 4 000 m in depth) at room temperature (about 20 °C). The other two samples were heated to 150 °C and 300 °C, at a rate of 10 °C per hour and the hydrostatic pressure of 100 MPa, respectively. Then the tests of rock fragmentation by cutting were carried out after the temperature and pressure were remained to be unchanged for 7–10 hours. The ordinary PDC bit, 30 mm in diameter, applied to cutting and breaking rock, was connected with six-edge poles by thread. The rock debris was flushed off the borehole by water flow.

All granite samples for borehole stability experiments were heated to target temperature at a rate of 5 °C per hour, and then the preset pressure was loaded on them based on loading scheme of temperature and pressure (Table 1). Creep test lasted for at least 48 hours at each

Table 1 Testing parameters.

Stage	Temperature (°C)	Pressure (MPa)	Depth (m)
A	20–150	12.5	500
B	150–200	25	1 000
C[c]	200	25	1 000
D[c]	200	50	2 000
E	200–250	50	2 000
F[c]	250	50	2 000
G	250–300	50	2 000
H[c]	300	75	3 000
I[c]	400	100	4 000
J[c]	500	125	5 000
K	Fractured		

Note: The superscript “c” represents creep test.

stage. The axial and lateral deformations of rock were automatically recorded by computer. The displacement of borehole was observed and measured by the optical apparatus every hour.

3.3 Results of cutting fragmentation for granite at HTHP

The relations among rotating rate, BP and temperature of cutting fragmentation at various temperatures and constant hydrostatic pressure of 100 MPa are given in Fig.9. The effect of BP and temperature on the unit rock-breaking energy consumption (UREC) is shown in Fig.10.

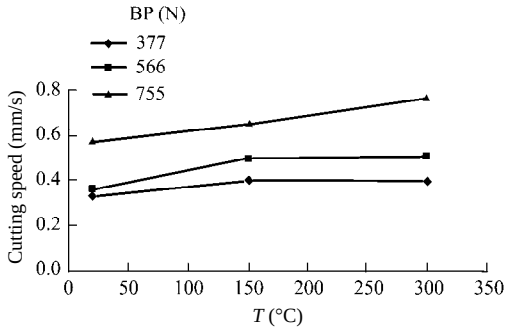

(a) Effect of BP and temperature on cutting speed at a rotating speed of 15 r/min.

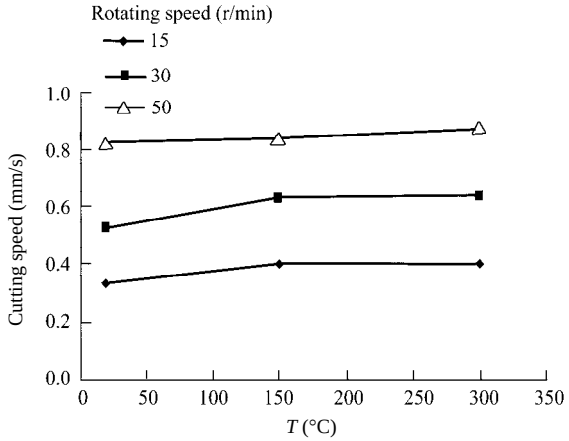

(b) Effect of rotating speed and temperature on cutting speed at a BP of 377 N.

Fig.9 Relations of rotational speed, bit pressure and temperature on cutting speed.

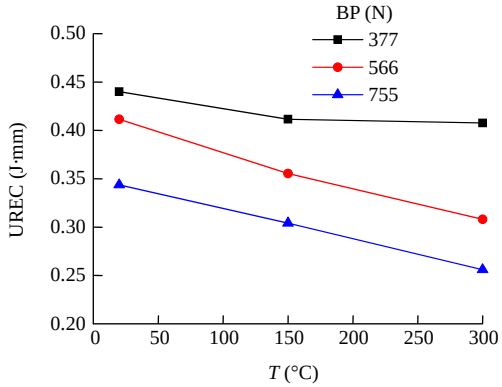

Fig.10 Effect of BP and temperature on UREC at a rotating speed of 15 r/min.

The machinability of granite increases gradually with increasing temperature at the hydrostatic pressure of 100 MPa, and the cutting speed obviously increases with increasing temperature when the BP is over a certain value. The cutting speed increases by 30%–50% at 300 °C, compared with that at room temperature, when the BP is 755 N. It is also believed that the brittle deformation of granite gradually transforms into ductile deformation with increasing temperature.

The UREC was calculated by broken rock volume (V_r) divided by driller work (W). The UREC decreases with increasing temperature at the hydrostatic pressure of 100 MPa while the efficiency of breaking rock increases. The UREC decreases by 20%–40% at 300 °C and BP of 755 N compared with that at room temperature in Fig.10. The reason may be that the intercrystalline microcracks induced by temperature result in the decrease in tensile strength.

The regulations that the cutting speed increases with the rotating speed or BP and the UREC increases with increasing rotating speed but reduces with increasing BP at HTHP are basically consistent with those at room temperature without confining pressure. If the BP is low, the effect of temperature on the cutting speed and UREC will be reduced since granite is damaged gradually and its compressive strength reduces slowly at the temperature of 300 °C and hydrostatic pressure of 100 MPa. Therefore, in order to obtain a good cutting of boring effect in granite at high temperature, the BP should exceed a certain value.

3.4 Borehole stability of granite at HTHP

3.4.1 *Borehole deformation of granite at HTHP*

The complete deformation of borehole in the second rock sample at high temperature ($T \leq 600$ °C) and high pressure ($P \leq 150$ MPa) is shown in Fig.11. It is illustrated that the displacement of borehole gradually increases with increasing temperature and pressure. The complete deformation could be categorized into three sections.

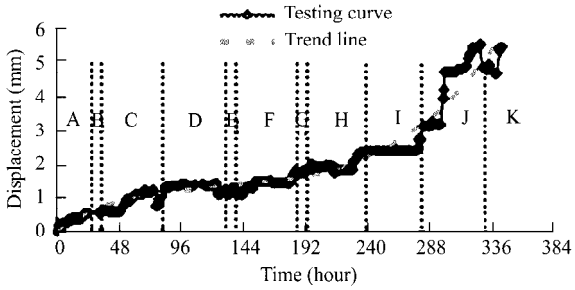

Fig.11 Complete curves of borehole deformation at HTHP.

In the first section, the deformation of borehole wall steadily increases at temperature less than 400 °C and hydrostatic pressure less than 100 MPa. Fig.12 shows the detailed time-dependent deformation in the first section. The diameter of borehole reduces slowly at constant temperature and pressure. The maximum displacement of borehole reaches 1.88 mm and the maximum strain is 1.88% in this section.

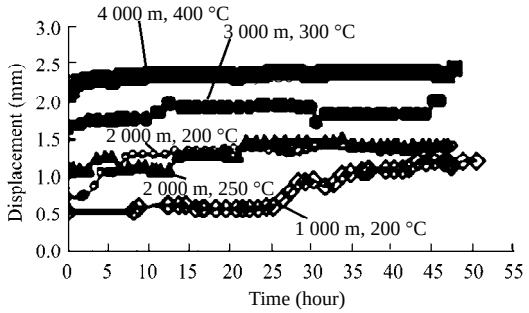

Fig.12 Displacement curves of borehole at $T \leq 400$ °C and $P \leq 100$ MPa.

In the second section, where the deformation drastically increases, the temperature ranges from 400 °C to 500 °C and hydrostatic pressure from 100 to 125 MPa. A remarkably fast creep is observed in the second section. The borehole diameter decreases to 30 mm at the temperature of 500 °C and hydrostatic pressure of 125 MPa. The maximum creep strain reaches 5% (Fig.13). The fluctuation of creep strain in Fig.13 results from the effect of small pieces dropping down from the borehole wall on the borehole diameter.

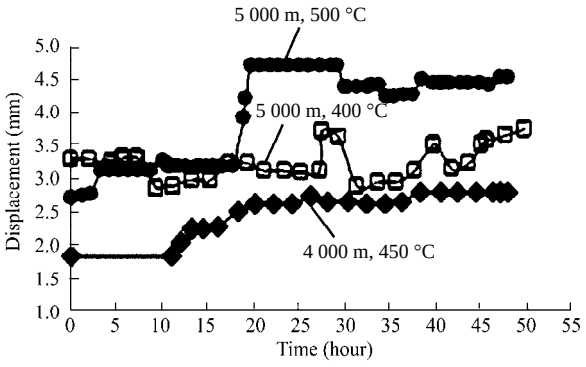

Fig.13 Displacement curves of borehole at T = 400 °C–500 °C and P = 100–125 MPa.

Borehole collapses in the last section at temperature exceeding 500 °C and pressure greater than 125 MPa. The creep rate is shown in Fig.14. The deformation comes into fast creep while the creep rate reaches 8.3×10^{-6} per hour at 400 °C and 100 MPa. When it increases to 16.9×10^{-6} per hour, the borehole will be broken.

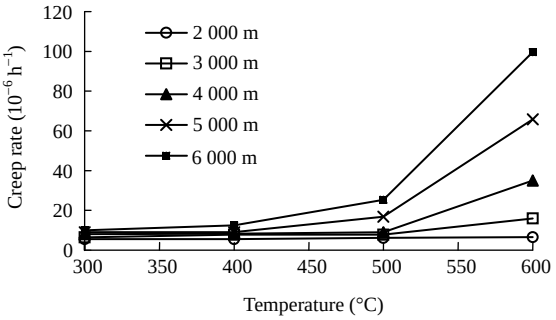

Fig.14 Creep rate at different temperatures and pressures.

3.4.2 *Damage characters and critical instability condition of borehole*

A few of small pieces dropped down from the borehole wall and then the borehole collapse occurred at $T \geq 500$ °C and $P \geq 125$ MPa. The damage state was recorded by camera and a video through borehole infrared imaging instrument (BIII), as shown in Fig.15. The borehole was not necking gradually, as shown in Fig.15, but expanded in diameter due to the drop of small pieces from borehole wall. The granite is a hard brittle rock and the borehole diameter in granite reduces slowly owing to creep. Simultaneously, thermally induced cracks are connected with each other and a few of free unsteady small pieces are formed.

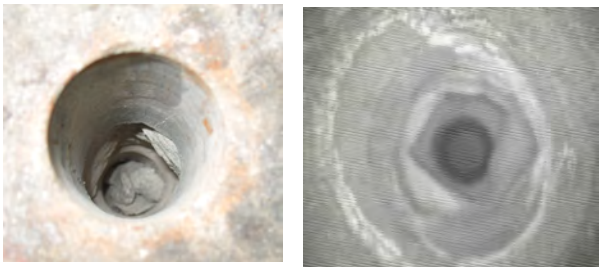

(a) Image recorded by camera. (b) Image recorded by BIII.

Fig.15 Pictures of borehole failure in granite.

The borehole diameter after testing was measured in axial direction, as shown in Fig.16. It indicates that the borehole diameter begins to increase at the point 109 mm away from the bottom and stops at the point 95 mm away from the other end. The drastically damaged section, whose maximum diameter is 52 mm, is 190–200 mm away from the bottom end.

Compression-shear damage is the main failure pattern of granite with a preset borehole. The final failure of granite appears at T = 550 °C–630 °C and P = 125–150 MPa (Table 2).

The critical temperature and pressure, which result in an intensive damage to granite, are 400 °C–500 °C and 100–125 MPa, respectively, from all above-mentioned results. The creep deformation drastically

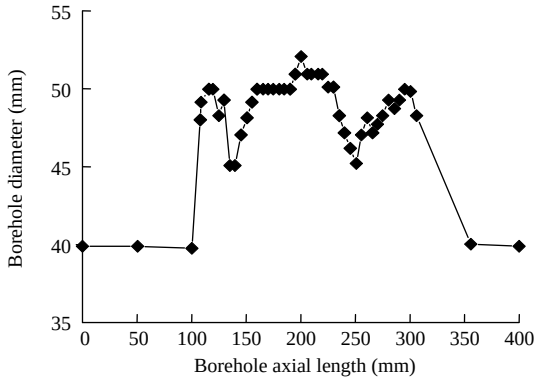

Fig.16 Relation between diameter and axial length of borehole No.2.

Table 2 Critical temperature and stress of granite failure.

Sample No.	Testing time (hour)	Ground depth (m)	Temperature (°C)	Stress (MPa)	Failure pattern
1	410.5	6 000	550	150	Compression-shear
2	344.0	5 000	600	125	Compression-shear and compression
3	140.5	6 000	630	150	Compression-shear and compression

increases and the borehole collapse happens under this condition.

3.5 The effect of thermal cracking on rock breaking and borehole stability

The granite, composed of many minerals such as quartz and feldspar, is a crystal rock. Thermal cracking will occur along the boundary of grain or across the grain. It will result in the decrease in rock strength and influence the deformation [25]. Therefore, thermal cracking is in favor of rock breaking and induces borehole instability. The experimental results from tests of cutting fragmentation show that the cutting speed will increase with temperature up to 300 °C. It can be inferred that rock-breaking will be easier at higher temperature compared with that at 300 °C. But according to the results of borehole stability analysis, the borehole will collapse at the temperature of 500 °C and the confining pressure of 125 MPa. The collapse will significantly influence the engineering scheme. If the effect of drilling fluid on the wall is considered in practice, the critical temperature and pressure of borehole instability may be lower than those in the present experiment.

4 Conclusions

In order to propose a scientific scheme on HDR geothermal energy exploitation in the Yangbajing basin, Tibet, China, the temperature distribution and the characters of geological structure were analyzed, and a series of experiments on drilling at HTHP using self-developed 20 MN servo-controlled triaxial rock testing machine were conducted.

A huge heat producer induced by a high-temperature liquating magma exists in the Yangbajing geothermal field. The calculated results of temperature distribution in this region by finite element method show that the geothermal gradient is about 45 °C/km and the estimated HDR geothermal resources in the Yangbajing region is 4.73×10^{13} kW·h. The results of measured crustal stress and focal mechanism solution show that the minor horizontal principal stress in the Yangbajing geothermal field is perpendicular to the basin strike and the maximum horizontal principal stress is parallel to it.

The design of mining plan of HDR geothermal resources was proposed. Considering the fault sliding zone, which is in the vicinity of the high-temperature liquating rock region, as an artificial reservoir, the vertical injection well was drilled in the lower site along the lean direction of the fault, while the lean production wells were in the higher site. The artificial reservoir volume is 3×10^{11} m^3 and a power station with a capacity of 10^4 MW operating for 100 years can be built. According to the analysis of the geothermal extraction system, which consists of one injection well and two production wells mentioned in this plan, a power station with a capacity of 1 000 MW can be considered in the initial period and the total electric production will reach 8.64×10^9 kW·h per year.

The machinability of granite increases gradually with increasing temperature at the pressure of 100 MPa, and the cutting speed obviously increases with increasing temperature when the BP is over a certain value. The UREC decreases and the efficiency of rock-breaking increases with increasing temperature at the pressure of 100 MPa, and the brittle deformation of granite gradually transforms into ductile deformation with increasing temperature.

The complete deformation of borehole in the granite could be divided into three sections: steady increasing, drastic increasing, and borehole collapse at various temperatures and pressures.

Compression and shear damages are the main failure patterns of granite with a preset borehole. The final failure of granite appears at the temperature of 500–600 °C and the pressure of 125–150 MPa. The critical temperature and pressure resulting in intensive damage to granite are 400–500 °C and 100–125 MPa,

respectively.

References

[1] Duchane D V. Status of the United States hot dry rock geothermal technology development program. Geothermal Technology, 1994, 19 (1/2): 12–30.

[2] Duchane D V. Hot dry rock: a realistic energy option. Geothermal Resources Council Bulletin, 1990, 19 (3): 83–88.

[3] New Energy and Industrial Technology Development Organization (NEDO). Report on the status of geothermal energy research in Japan (1980–1989). Tokyo: New Energy and Industrial Technology Development Organization (NEDO), 1991.

[4] Zhao Yangsheng, Wan Zhijun, Kang Jianrong. Introduction to geothermal extraction of hot dry rock. Beijing: Science Press, 2004 (in Chinese).

[5] Yao Dongchun. Drill geothermal well with new style PDC aiguilles. Foreign Petroleum Machinery, 1995, 6 (4): 10–17 (in Chinese).

[6] Tian Zhikun. The aiguilles of design to terrestrial heat make hole. Exploration Engineering (Drilling and Tunneling), 1989, (6): 64–66 (in Chinese).

[7] Zhao Fujun, Li Xibing, Feng Tao, Xie Shiyong. Theoretical analysis and experiments of rock fragmentation under coupling dynamic and static loads. Chinese Journal of Rock Mechanics and Engineering, 2005, 24 (8): 1 315–1 320 (in Chinese).

[8] Tezuka K, Niitsuma H. Stress estimated using microseismic clusters and its relationship to the fracture system of the Hijiori hot dry rock reservoir. Engineering Geology, 2000, 56 (1/2): 47–62.

[9] Cornet F H, Bérard Th, Bourouis S. How close to failure is a granite rock mass at a 5 km depth?. International Journal of Rock Mechanics and Mining Sciences, 2007, 44 (1): 47–66.

[10] Haimson B C, Chang C. True triaxial strength of the KTB amphibolite under borehole wall conditions and its use to estimate the maximum horizontal in-situ stress. Journal of Geophysical Research, 2002, 107 (B10): 1–15.

[11] Liang Lixi, Xu Qiang, Liu Xiangjun. Quantitative evaluation of well wall stability based on the theory of limit equilibrium. Petroleum Drilling Techniques, 2006, 34 (2): 15–17 (in Chinese).

[12] Haimson B. Micromechnisms of borehole instability leading to breakouts in rocks. International Journal of Rock Mechanics and Mining Sciences, 2007, 44 (2): 157–173.

[13] Duo Ji. The basic characteristics of the Yangbajing geothermal field—a typical high temperature geothermal system. Engineering Science, 2003, 5 (1): 42–47 (in Chinese).

[14] Zhao Wenjin, Wu Zhenhan, Shi Danian, Xiong Jiayu, Xue Guangqi, Su Heping, Hu Daogong, Ye Peisheng. Comprehensive deep Profiling of Tibetan Plateau in the INDEPTH Project. Acta Geoscientica Sinica, 2008, 29 (3): 328–342 (in Chinese).

[15] Wan Zhijun, Zhao Yangsheng, Kang Jianrong. Simulation and forecast method of geothermal resources in hot dry rock. Chinese Journal of Rock Mechanics and Engineering, 2005, 24 (6): 945–949 (in Chinese).

[16] Wu Zhenhan, Barosh P J, Zhao Xun, Wu Zhonghai, Hu Daogong, Liu Qisheng. Miocene tectonic evolution from dextral-slip thrusting to extension in the Nyainqentanglha region of the Tibetan Plateau. Acta Geologica Sinica, 2007, 81 (3): 365–384.

[17] Zhang Chunshan, Wu Manlu, Liao Chunting, Ma Yinsheng, Ou Mingyi. The result of current stress measurements and stress state analysis in the region of Yangbajing-Kangmar in Tibet. Chinese Journal of Geophysics, 2007, 50 (2): 517–522 (in Chinese).

[18] Xu Jiren, Zhao Zhixin, Ishikawa Y. Extensional stress field in the central and southern Qinghai-Tibetan plateau and dynamic mechanism of geothermic anomaly in the Yangbajing area. Chinese Journal of Geophysics, 2005, 48 (4): 861–869 (in Chinese).

[19] Brown D W. Update on the long-term flow testing program. In: Proceedings of Geothermal Energy and the Utility Market—the Opportunities and Challenges for Expanding Geothermal Energy in a Competitive Supply Market. San Francisco: [s.n.], 1992: 159–164.

[20] Tester J W. testimony on hot dry rock geothermal energy. Geothermal Resources Council Bulletin, 1992, 21 (5): 137–147.

[21] Parker R H. Hot dry rock geothermal energy, phase 2B—final report of the Camborne School of Mines Project. London: Pergamon Press, 1989.

[22] Marechal J C, Perrcochet P, Tacher L. Long-term simulations of thermal and hydraulic characteristics in mountain, mass of the Mont Blance case study in French and Italian Alps. Hydrogeology Journal, 1999, 7 (4): 341–354.

[23] Pierce K G. An estimation of the cost of electricity production from hot dry rock. Geothermal Resources Council Bulletin, 1993, 22 (8): 197–203.

[24] Bai Taixu, Wang Shengzu. Numerical modeling of stress distribution in rock specimen under triaxial compression with solid confining medium. Chinese Journal of Rock Mechanics and Engineering, 1990, 9 (2): 154–163 (in Chinese).

[25] Wan Zhijun, Zhao Yangsheng, Dong Fuke, Feng Zijun, Zhang Ning, Wu Jinwen. Experimental study on mechanical characteristics of granite under high temperature and triaxial stresses. Chinese Journal of Rock Mechanics and Engineering, 2008, 27 (1): 72–77 (in Chinese).